Journal of Materials Processing Technology 210 (2010) 2103–2118

Contents lists available at ScienceDirect

Journal of Materials Processing Technology

journal homepage: www.elsevier.com/locate/jmatprotec

A review on hot stamping

H. Karbasian*, A.E. Tekkaya

Institute of Forming Technology and Lightweight Construction, Dortmund University of Technology, Baroper Str. 301, D-44227 Dortmund, Germany

ARTICLE INFO

Article history:
Received 29 October 2009
Received in revised form 15 July 2010
Accepted 19 July 2010

Keywords:
Hot stamping
High strength steel
22MnB5

ABSTRACT

The production of high strength steel components with desired properties by hot stamping (also called press hardening) requires a profound knowledge and control of the forming procedures. In this way, the final part properties become predictable and adjustable on the basis of the different process parameters and their interaction. In addition to parameters of conventional cold forming, thermal and microstructural parameters complicate the description of mechanical phenomena during hot stamping, which are essential for the explanation of all physical phenomena of this forming method.

In this article, the state of the art in the thermal, mechanical, microstructural, and technological fields of hot stamping are reviewed. The investigations of all process sequences, from heating of the blank to hot stamping and subsequent further processes, are described. The survey of existing works has revealed several gaps in the fields of forming-dependent phase transformation, continuous flow behavior during the whole process, correlation between mechanical and geometrical part properties, and industrial application of some advanced processes. The review aims at providing an insight into the forming procedure backgrounds and shows the great potential for further investigations and innovation in the field of hot sheet metal forming.

1. Introduction

Due to the demand for reduced vehicle weight, improved safety, and crashworthiness qualities, the need to manufacture automobile structural components from ultra high strength steels is apparent (Åkerström, 2006). Hot stamping was developed and patented (GB1490535, 1977) by a Swedish company (Plannja), that used the process for saw blades and lawn mower blades. In 1984 Saab Automobile AB was the first vehicle manufacturer who adopted a hardened boron steel component for the Saab 9000 (Berglund, 2008). The number of produced parts increased from 3 million parts/year in 1987 to 8 million parts/year in 1997. Since the year 2000 more hot stamped parts have been used in the cars and the number of produced parts/year has gone up to approximately 107 million parts/year in 2007 (Aspacher, 2008). The applied hot stamped parts in the automotive industry are chassis components, like A-pillar, B-pillar, bumper, roof rail, rocker rail and tunnel (Fig. 1).

The hot stamping process currently exists in two different main variants: the direct and the indirect hot stamping method. In the direct hot stamping process, a blank is heated up in a furnace, transferred to the press and subsequently formed and quenched in the closed tool (Fig. 2a). The indirect hot stamping process is characterized by the use of a nearly complete cold pre-formed part which is subjected only to a quenching and calibration operation in the press after austenitization (Fig. 2b) (Merklein et al., 2008). Full martensite transformation in the material causes an increase of the tensile strength of up to 1500 MPa.

This paper includes the review over the research on hot stamping. This starts with the description of the workpiece material used in hot stamping. Then, the special characteristics of the process steps in the process chain of hot stamping are described. Finally, the subsequent processing of the hot stamped parts and the manufacture of the parts with tailored properties are presented. The paper includes both the experimental and numerical investigations in the field of hot stamping.

2. Material and coating

The investigations on ultra high strength steels by Naderi have shown that boron alloys of 22MnB5, 27MnCrB5, and 37MnB4 steel grades (Table 1) are the only steel grades which produce a fully martensitic microstructure after hot stamping when a water-cooled tool is used (Naderi, 2007). Here, 22MnB5 steel grade is the most commonly used steel grade in hot stamping processes. Initially, the material exhibits a ferritic–pearlitic microstructure with a tensile strength of about 600 MPa. After the hot stamping process, the component finally has a martensitic microstructure with a total strength of about 1500 MPa (Fig. 3a). In order to achieve such a microstructure and hardness transformation, the blank has

* Corresponding author. Tel.: +49 231 7557430; fax: +49 231 7552489.
E-mail address: Hossein.Karbasian@iul.tu-dortmund.de (H. Karbasian).

0924-0136/$ – see front matter © 2010 Published by Elsevier B.V.
doi:10.1016/j.jmatprotec.2010.07.019

Table 1
Chemical components and mechanical properties of boron steels (Naderi, 2007).

Steel	Al	B	C	Cr	Mn	N	Ni	Si	Ti
20MnB5	0.04	0.001	0.16	0.23	1.05	–	0.01	0.40	0.034
22MnB5	0.03	0.002	0.23	0.16	1.18	0.005	0.12	0.22	0.040
8MnCrB3	0.05	0.002	0.07	0.37	0.75	0.006	0.01	0.21	0.048
27MnCrB5	0.03	0.002	0.25	0.34	1.24	0.004	0.01	0.21	0.042
37MnB4	0.03	0.001	0.33	0.19	0.81	0.006	0.02	0.31	0.046

Steel	Martensite start temperature in °C	Critical cooling rate in K/s	Yield stress in MPa		Tensile strength in MPa	
			As delivered	Hot stamped	As delivered	Hot stamped
20MnB5	450	30	505	967	637	1354
22MnB5	410	27	457	1010	608	1478
8MnCrB3	–*	–*	447	751	520	882
27MnCrB5	400	20	478	1097	638	1611
37MnB4	350	14	580	1378	810	2040

* There is no possibility to have fully martensitic microstructure.

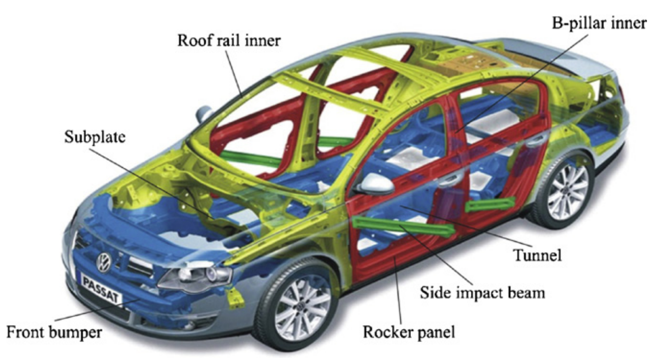

Fig. 1. Hot stamped parts in a typical middle class car (N. N., 2009).

to be austenitized in a furnace for at least 5 min at 950 °C. Afterwards, the blank is formed and quenched simultaneously by the water-cooled die for 5–10 s. Due to the contact between the hot blank and the cold tool, the blank is quenched in the closed tool. If the cooling rate exceeds a minimum cooling rate of approximately 27 K/s, at a temperature of around 400 °C, a diffusionless martensitic transformation will be induced, which finally is responsible for the resulting high strength of the part (Fig. 3b) (Merklein et al., 2008). The martensite transformation begins at 425 °C (martensite start point M_s) and ends at 280 °C (martensite finish point M_f) (Somani et al., 2001).

The mechanical properties of steel after quenching change in dependence on its carbon content and consequently, the strength after quenching can be controlled by a proper adjustment of the carbon content. The alloying elements, such as Mn and Cr, are known to have only a small influence on the strength after quenching. However, since these elements have an influence on hardenability, they are essential for shifting of existence fields. Thus, the desired phase transformation and hardenability is achieved by technically feasible cooling rates (Garcia Aranda et al., 2002). Boron is the element which influences the hardenability the most, whereas boron slows down the conversion into softer microstructures and leads to a martensitic microstructure over the cross-section of the part.

Under austenitization conditions, oxide scale formation occurs immediately when the steel is in contact with air. In order to avoid surface oxidation and decarburization, most sheet metal blanks are pre-coated with a protective layer. The widespread protection is an Al–Si layer preventing scale formation on the steel during the direct hot stamping operation. Borsetto et al. (2009) investigated the influence of thermal process parameters on the chemical behavior of the coating of the Al–Si layer. This metallic coating is generated in a continuous hot-dip galvanizing process and consists of 10% silicon, 3% iron, and 87% aluminum. During the heating of the coated blank, the steel diffusion process from the coating–substrate interface area to the coating surface is thermally activated. The Al–Si coating has a melting point of approximately 600 °C. However, due to the presence of Fe in the substrate, an Al–Fe alloy with a higher melting point grows from the interface with the base metal and quickly reaches the surface. The Al–Fe alloy, which migrates to the surface, has a higher melting point and this prevents the coating layer from melting. For a heating temperature of 950 °C typical of hot stamping processes, a sub-layer structure characterized by

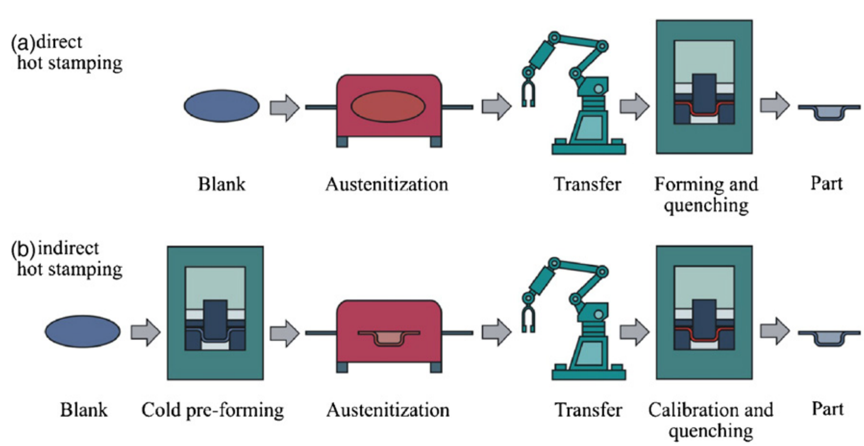

Fig. 2. Basic hot stamping process chains: (a) direct hot stamping, (b) indirect hot stamping.

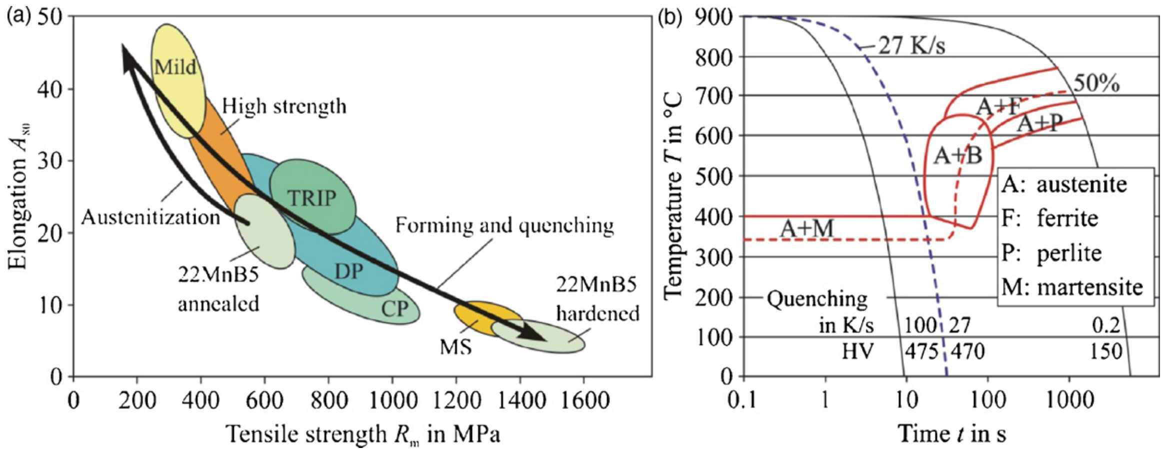

Fig. 3. Mechanical properties of 22MnB5 and CCT diagram (Garcia Aranda et al., 2002).

an alternating variation of the chemical Al–Fe percentages appears (Borsetto et al., 2009). In the direct hot stamping process, this protective layer prevents the formation of scales. Due to the lower forming limits of the Al–Si layer compared to the base material in the initial state at room temperature, the hot-dip aluminized sheets cannot be used for the indirect process and they are not suitable for cold forming. This coating does not provide cathodic protection, like zinc, but a high barrier protection. Similar to cold formed parts, a cathodic protection is desirable for hot stamped components. These demands of the automotive industry could be met by metallic coatings with cathodic protection, e.g. zinc. During heating and hot stamping, the hot-dip galvanized zinc layer reacts with the base material to form intermetallic zinc–iron-phases. In order to minimize the propagation of microcracks in the coating layer into the base material, hot-dip galvanized 22MnB5 can only be used for indirect hot stamping. After hot stamping, the oxide layer must be removed by shot peening to avoid a bad paint adherence. Another established protective coating for 22MnB5 is x-tec® (Goedicke et al., 2008) which is applied as a varnish in a coil coating process for the direct and indirect hot stamping process with additional active corrosion protection. This coating is based on the combination of μm-scaled materials according to the sol–gel process. Inorganic and organic materials are linked together and blended with aluminum particles to form a protective coating. The tribological behavior of this 7 μm thick protective coating in the cold forming operation allows a controllable material flow without additional lubrication (Paar et al., 2008).

The latest method for the prevention of oxidation involves coating the sheets with preventive oil, as described in the work of Mori and Ito (2009). The oxidation of heated sheets in an electrical furnace could be prevented and the effect of two different oils was studied. The effect of the oxidation preventive oil was evaluated in a cooling experiment without forming and in a hot bending experiment. The analysis of the sheet surface has shown that the number of lubrications (up to 4 times) reduces the surface oxidation.

3. Heating

The hot stamping process begins with the heating of the blank up to the austenitization temperature. For the determination of the process window regarding a homogeneous austenitization of the blanks during hot stamping as a pre-condition for the desired fully martensitic transformation, annealing tests were performed by Lechler and Merklein (2008) considering austenitization temperature and time. In these tests, the samples were quenched through a full metallic contact pressure of 40 MPa on both sides. To evaluate the occurring phase transformations, the hardness of the quenched blanks were measured according to Vickers HV10. The minimum austenitization time at different austenitization temperatures and different sheet thicknesses to achieve the maximum hardness of 470 HV are shown in Fig. 4.

The results of this study show the significant dependency of the austenitization temperature (Fig. 4a) and the sheet thickness (Fig. 4b) on the minimum heat treatment time with respect to a homogenous austenitization of the quenchable steel 22MnB5. At a furnace temperature of 950 °C, a dwell time of 3 min was found to be sufficient to obtain the maximum martensitic content in the quenched samples with a maximum hardness of approximately 470 HV. With decreasing furnace temperature, the austenitization duration time increases. The upper time limit of Al–Si pre-coated blanks is determined by means of the thickness of the alloying ternary Al–Si–Fe layer (Austerhoff and Rostek, 2002) during heat treatment with the objective to ensure a sufficiently accurate weldability (Stopp et al., 2007) of the hot stamped parts during post processing. According to the experiences from industry (Stopp et al., 2007), a layer thickness of approximately 40 μm should not be exceeded during austenitization in the furnace.

The investigations of Lechler (2009) have shown that the heating procedure of the blank has a great influence on the part properties, the process time, and the cost-efficiency of hot stamping. Therefore, a homogenous blank temperature and a short heating time are the main demand on the heating system. The blank can be heated using different thermal phenomena: radiation in a furnace, induction, and conduction (Fig. 5).

3.1. Roller hearth furnace

On the existing lines, the blank is usually heated in roller heath furnaces or walking beam furnaces. The size and connected load of these furnaces depend on the through-put and the material to be heated. Al–Si coated materials used for preventing scale formation require a special heating curve due to a necessary diffusion process between base material and the coating (Suehiro et al., 2003).

The furnaces of the existing hot stamping lines already reach lengths of 30–40 m. The high space requirement and the rising investment costs show the need for alternative approaches to heat the blanks.

The cycle time for press-hardened parts is mainly dependent on the die closing time and the furnace residence time required to austenitize the material and, in the case of coating, to achieve the required through-alloying. With regard to die closing time, optimization of die cooling or the tool steels used could provide a reduction in cycle time. A reduction in furnace residence time can

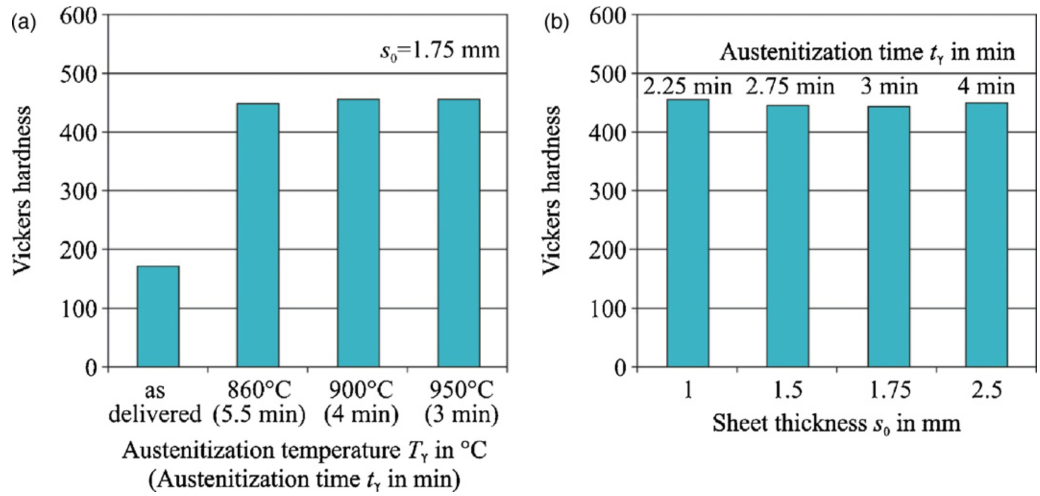

Fig. 4. Influence of austenitization temperature, time (a), and sheet thickness (b) on the minimum austenitization time to achieve the maximum hardness of 470 HV (Lechler and Merklein, 2008).

only be achieved by the following faster heating concepts (Lenze et al., 2008a,b). These methods are in the development phase, and laboratory investigations must verify them for industrial application.

3.2. Conduction heating

An alternative heating system is conduction heating. For the heating process, a blank is clamped between the two pairs of electrodes (Mori et al., 2009). The current flows through the sheet metal part. The resistance of the material causes the heating of the part. The conduction heating of the metallic substances is based on Joule's Law, according to which the heat generated in an electric circuit is proportional to the power of the electric circuit. The loss of power due to the electrical resistance of the conductors results in the conductors themselves being heated. A low surface quality and insulating pollution layers on the component increase the resistance and thus the heat generation in the contact area. The design of these contacts and the control of the contact pressure are critical for the homogenous heating of the component (Kolleck et al., 2008).

An important basis for the use of conduction heating is the efficiency factor. This parameter directly depends on the part's resistance. Because of the higher resistance of long components in comparison to short components, conduction heating is mainly used for components with a favorable length/diameter ratio, such as pipes, rods, wires, and bands (Kolleck et al., 2008). Disadvantage of this heating system is the inhomogeneous temperature along the length of the component. Another problem for the industrial application of this heating method is the difficulty of heating blanks with complex geometries homogeneously (Behrens et al., 2008).

3.3. Induction heating

The last heating system is the inductive heating of the blank. In principle, all electrically conducting or semiconducting substances can be heated by induction, and the resulting area of application is correspondingly large for this technology: melting of metals, bulk forming and tempering, and assembly and packaging industry. The geometry of the inductor determines the position of the magnetic field relative to the workpiece, which causes different degrees of efficiency. The distance between inductor and sheet also has an influence on the efficiency of the heating system. On the one hand, the electrical insulation between inductor and sheet must be guaranteed; on the other hand, shaped blanks tend to go out of shape while being heated. A small distance to the inductor can cause the jamming of the heated blank with the risk of damaging the heating system (Kolleck et al., 2009a,b). Compared to roller heath furnaces, the energy efficiency of induction heating is up to two times higher, because of the higher losses of the roller heath furnace by exhaust gases and the rollers.

4. Forming

In order to avoid cooling of the part before forming, the blank must be transferred as quickly as possible from the furnace to the press. Furthermore, forming must be completed before the beginning of the martensite transformation. Therefore, a fast tool closing

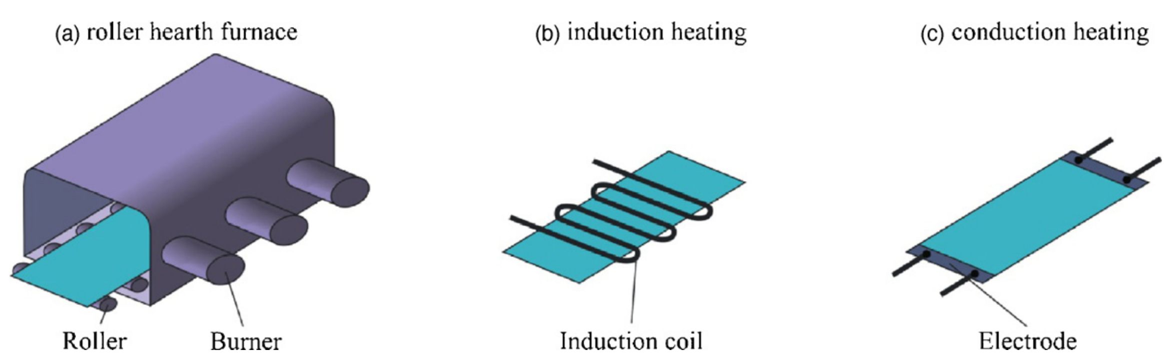

Fig. 5. Heating systems: (a) roller hearth furnace, (b) induction heating, (c) conduction heating.

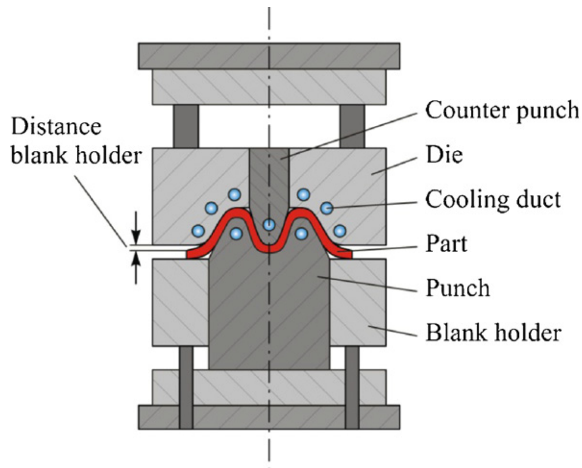

Fig. 6. Tool design for the hot stamping process.

and forming process are the precondition for a successful process control. After forming, the part is quenched in the closed tool, which is cooled by water ducts to transfer the heat out of the tool system. In order to avoid the quenching of the blank between the blank holder and the die during the forming process, most of the hot stamping tool systems work with a distance blank holder (Fig. 6).

Another process variant is hot stamping by means of working media. The use of temperature as a process parameter in hot gas forming and a simultaneous quenching of the formed parts offer the opportunity to increase the application field of this innovative technology (Neugebauer et al., 2009). The forming procedure starts with the positioning of the profile or the blank. After the tool is closed, the forming step is performed using the working media (Fig. 7). In the work of Neugebauer et al. (2009), nitrogen, and in the work of Lindkvist et al. (2009), air is used as the working medium with a pressure of up to 600 bar. The advantage of hot gas forming in comparison to conventional hot stamping is the free forming of the part at the beginning of the forming process. In addition, because of the lower contact time between the part and the tool during forming, a homogenous blank temperature distribution leads to a uniform forming of the blank. Another interesting field in gas forming may be the application of thermally insulating and/or incompressible working media.

The current strong demand for a higher efficiency of hot sheet metal forming processes inevitably leads to the question of how to shorten the process cycle. Cooling can be accelerated by the application of tool steels with improved heat conductivity (Casas et al., 2008) and/or more efficient cooling systems (Hoffmann et al., 2007). By the application of the tool steels developed by Casas et al. (2008) with a thermal conductivity of up to 66 W/mK, the holding time could be reduced from 10 to 2 s.

4.1. Cooling ducts

The quenching operation during the hot stamping process does not only influence the economy of the process but also the final properties of the component. The objective of the cooling ducts design is to quench the hot part effectively and to achieve a cooling rate of at least 27 K/s while martensite forms. The die cooling system is economical if a fluid coolant, such as water, is used, which flows through cooling ducts around the contours of the component. The heat flow in the formed component is dependent on the heat transfer from the component to the tool, the heat conductivity within the tool, and the heat transfer from the tool to the coolant. For an optimum heat transfer between component and tool, the contact surface should not exhibit a scale or a gap. The heat conductivity within the tool can be considerably influenced by the choice of the tool material. Another important factor with respect to heat drain is the design of the cooling ducts, which is defined by the size, location, and distribution of the cooling ducts. The heat drain can be accelerated by using a coolant with a low temperature in order to increase the temperature difference between the coolant and the tool and therefore the resulting heat flux (Steinbeiss et al., 2007).

The cooling holes can be drilled in the forming tool. For this method, the machining restrictions should be considered in the design of the hole position (Steinbeiss et al., 2007). Therefore, an optimal design of the cooling system as to heat transfer is not possible. Another alternative is to provide the cooling holes as pipes in the casting mold of the tool (Kuhn and Kolleck, 2006). The unrestricted design of the cooling system is the advantage of this method. Alternatively, the tools can be manufactured using the lasered blank segments, which are screwed and form the tool surface with integrated cooling holes (Freieck, 2007). This method is very cost-effective, but the lamellar design can have negative effects on the part surface and the heat transfer within the tool.

4.2. Wear of the tool surface

The wear resistance of the tool has been measured by Dessain et al. (2008) using a strip drawing equipment which is adapted to high temperature tests. The resistance heating device allows heating up the Al–Si coated 22MnB5 strip. The heated strip slides over the die radius. For this test, the contact surface was made of abrasion and adhesion areas. The die abrasion was predominant and adhesion of Al–Si was observed at the end of the contact area with the blank. These built layers, formed very early at the beginning of the test, are known to form compacted layers on the tool surface during sliding of the strip (Hardell and Prakash, 2008) and exhibited low wear.

The exposure of the tool steel to high temperatures in a hot forming operation can result in large variations in friction due to changes in the surface topography, removal of oxide layers and excessive wear of the tool. One approach to overcome friction problems is to apply suitable surface treatments and/or coatings to the tool steel with. Tribological studies by Hardell and Prakash (2008) at room temperature and 400 °C on one plasma nitrided tool steel and two PVD coatings (CrN and TiAlN) sliding against UHSS were carried out using a pin-on-disc machine. The best results as to wear resistance were achieved by the TiAlN coating.

Comparable studies for another sheet coating do not exist. Furthermore, the austenitization time and its influence on the surface texture must be considered in design of experiments for further investigations.

5. Quenching

After the forming of the heated blank in the austenitic temperature range, the part is quenched in the closed tool until the entire martensite transformation of the part structure is completely. A cooling rate of more than 27 K/s is necessary for a full martensite microstructure of 22MnB5. Martensite evolution leads to an increase of the flow stress (Fig. 8). The transformation from austenite (fcc) into martensite (bct) causes an increase in volume, which influences the stress distribution during quenching. Only the complete description of the transformation behavior allows a prediction of the resulting material properties, the volume fraction of different phases, the residual stresses, and the distortion of the workpiece after cooling (Neubauer et al., 2008).

For the modeling of the thermoplastic transformation behavior, the strain increment can be described by the sum of elastic, plastic, thermal, and isotropic transformation and transformation-induced plasticity strains (Table 2). Due to the different lattice structures of

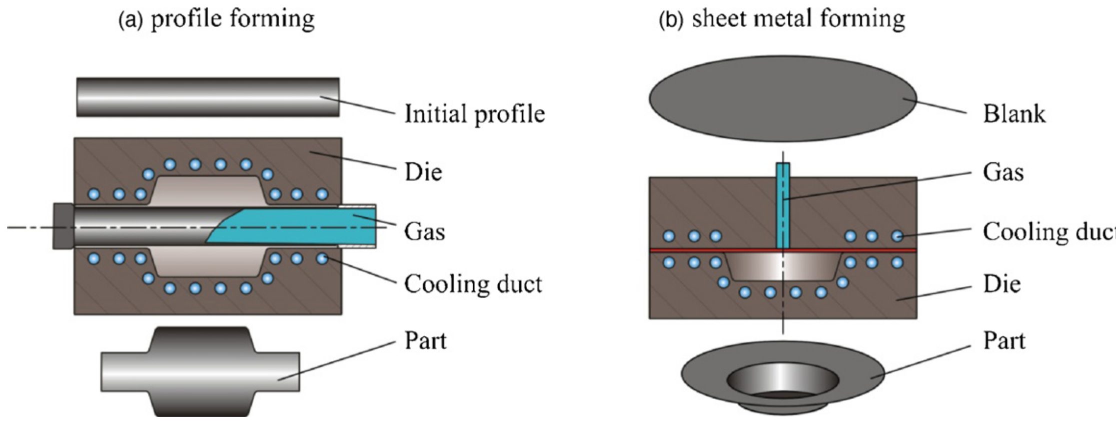

Fig. 7. Gas forming of profile (a) and sheet (b).

austenite and the resulting microstructures ferrite, pearlite, bainite and martensite, a volume change occurs during the phase transformation that can be described by means of the isotropic transformation strains. This effect causes only a change in volume, like the thermal strain increment. Additionally, the morphologies of these microstructural components are very different, and consequently their mechanical properties differ. Therefore, the study of material macroscopic behavior becomes a difficult homogenization problem due to the fact that new phases continuously evolve and the deformation history must be accounted for (Åkerström et al., 2007).

If the phase transformation occurs without applied stress, the material response is purely volumetric and an increase in volume is observed due to the compactness difference between the parent and product phase. When the transformations occur under an external stress, transformation-induced plasticity causes irreversible deformation. The Greenwood–Johnson mechanism (Greenwood and Johnson, 1965) describes the transformation plasticity which depends on the austenite and the resulting phase fraction. Therefore, micro-stresses are introduced that generate plastic strains in the austenite when deviatoric stress is applied. The commonly used model considering the transformation plasticity is the model by Leblond et al. (1989), which was further applied to numerical modeling by Åkerström (2006).

The described analytical model for the flow behavior can be verified using the continuous cooling transformation diagrams (CCT) under different forming modes. To determine the forming CCT diagram (FCCT), the heated specimen is formed until it reaches the test forming condition and is subsequently cooled at a predetermined rate. The degree of transformation is measured.

6. FE simulation

Hot stamping is a thermo-mechanical forming process with intended phase transformation. Depending on the temperature history and mechanical deformation, different phases and phase mixtures evolve. During the solid-state phase transformations, heat is released, which influences the thermal field. Furthermore, depending on the mixture of micro constituents, both the mechanical and thermal properties vary with temperature and deformation. Consequently, a realistic FE model for process simulation must consider interaction between the mechanical, thermal, and microstructural fields (Fig. 9). This requires process characteristics like the heat transfer coefficient, the material flow behavior, and the phase transformation under process-relevant conditions (Oldenburg, 2008). Due to the transfer of microstructural evolution data within the process simulation, final properties, such as hardness and tensile strength, can be properly modeled (Jeswiet et al., 2008).

For a consistent analysis of coupled thermo-mechanical deformations of metals, Ghosh and Kikuchi (1988) developed a finite element method, which models the flow behavior of metals at elevated temperatures. The proposed model considers the initial anisotropy and temperature dependence of metals for large-deformation forming processes.

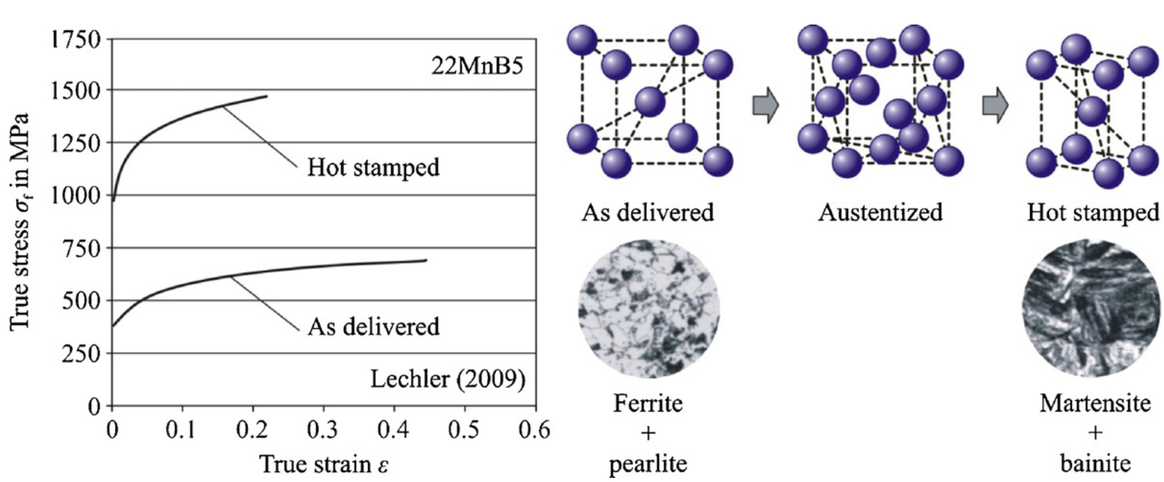

Fig. 8. Flow curves and microstructure of 22MnB5 during hot stamping.

Table 2
Strain rate components in hot stamping.

Total strain rate	$\dot{\varepsilon}_{ij} = \dot{\varepsilon}_{ij}^{el} + \dot{\varepsilon}_{ij}^{pl} + \dot{\varepsilon}_{ij}^{th} + \dot{\varepsilon}_{ij}^{tr} + \dot{\varepsilon}_{ij}^{tp}$ (1) ε_{ij}^{el}: elastic component, ε_{ij}^{pl}: plastic component, ε_{ij}^{tp}: trans. plasticity, ε_{ij}^{th}, ε_{ij}^{tr}: thermal and isotropic transformation component
Thermal and isotropic transformation component (Olle et al., 2008)	$d\varepsilon_{ij}^{th+tr} = d\varepsilon_{ij}^{th} + d\varepsilon_{ij}^{tr} = \left(\frac{a_n^{t+\Delta t}\left(T^{t+\Delta t}\right)}{a_n^t\left(T^t\right)} - 1 \right) \delta_{ij}$ (2) a_n: lattice constant, Δt: time step, δ_{ij}: Kronecker delta, T: temperature
Transformation plasticity rate (Åkerström, 2006)	$\dot{\varepsilon}_{ij}^{tp} = -\frac{3\Delta\varepsilon_{1-2}^{th} h\left(\frac{\bar{\sigma}}{\sigma^y}\right) \dot{z} \ln(z)}{\sigma_1^y\left(\bar{\varepsilon}_1^p, T\right)} s_{ij}$ (3) $h\left(\frac{\bar{\sigma}}{\sigma^y}\right) = \begin{cases} 1 & \frac{\bar{\sigma}}{\sigma^y} \le \frac{1}{2} \\ x + 3.5\left(\frac{\bar{\sigma}}{\sigma^y} - \frac{1}{2}\right) & \frac{\bar{\sigma}}{\sigma^y} > \frac{1}{2} \end{cases}$ $\Delta\varepsilon_{1-2}^{th}$: difference in compactness between austenite and the resulting phase, σ_1^y: current yield stress of austenite, z: volume fraction of resulting phase, s_{ij}: deviatoric stress, h: correction function according to the nonlinearity in the applied stress, $\bar{\sigma}$: current effective stress, σ^y: current global yield stress
Volume fraction of martensite (Koistinen and Marburger, 1959)	$z_M(t) = 1 - e^{\left(-a\left(T_{MS}-T\right)^{\kappa}\right)}$ (4) T_{MS}: martensite start temperature, a, κ: coefficients

In recent years, several concepts of coupling two FE programs specializing in their own respective domains for the performance of hot stamping have been developed. The coupled systems consider a thermal and a mechanical model, which are linked to achieve the transfer of geometrical and physical data. Because of the separate calculation of thermal and mechanical phenomena, the coupling concepts are very flexible and efficient for parameter adjustments within the FE models. The disadvantage of this method is the limited data transfer between the two FE models, which can influence the accuracy of the results of the simulation (Hein, 2005; Tekkaya et al., 2007). Another alternative for the FE simulation of hot stamping is the application of special purpose programs: LS-DYNA, AutoForm, and PamStamp. The FE models vary in the existing options for the definition and description of the physical processes. For example, the analysis with the FE software LS-DYNA can be performed using thermal shell elements coupled with mechanical shell elements for the metal sheet (Bergman and Oldenburg, 2004). The thermal problem is solved by the implicit time integration while the mechanical problem is processed by the explicit time integration method. This feature within LS-DYNA allows to combine the advantages of each integration rule and, at the same time, overcome contact solution stability and thermal convergence. The tools can be modeled as rigid bodies with thermal behavior (Karbasian et al., 2008a,b).

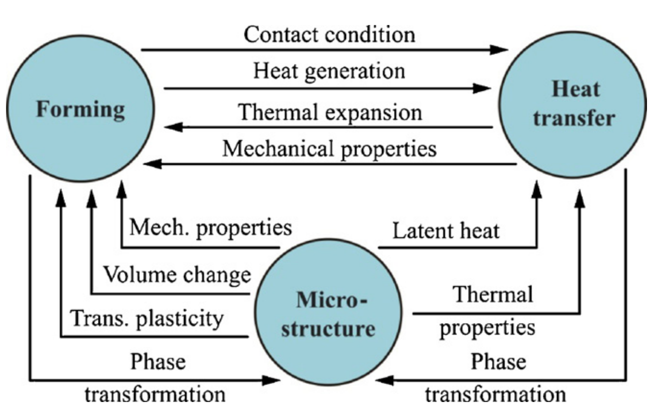

Fig. 9. Interaction between thermal, mechanical, and microstructural fields (Bergman, 1999).

The prediction of the temperature distribution in the blank and the tools plays a very important role in this process. A temperature-dependent hardening function is also required to characterize the plastic deformation and to take into account the heat between the blank and the tools as well as heat loss due to convection and radiation from the blank. The phase transformation from austenite to martensite must also be considered in order to simulate the hot forming process (Åkerström et al., 2007). In the following, the thermo-mechanical properties and their determination for the FE simulation of hot stamping are described.

6.1. Thermal characteristics

The prediction of the mechanical properties of hot stamped parts by means of FE simulation requires an accurate modeling of the thermal phenomena during forming and quenching. The heat transfer coefficient h is responsible for the thermal behavior and the respective cooling of the blanks throughout the whole forming operation and can be influenced by the contact pressure and the temperature of the steel sheet as well as the surface condition (scale thickness, roughness, coating thickness, etc.) (Forstner et al., 2007). As the mechanical properties of the base material 22MnB5 are strongly dependent on the temperature, this is one of the most important parameters to be taken into account regarding FE modeling of thermally assisted forming.

For the determination of the heat transfer coefficient, a quenching tool has been developed by Hoff (2007). The heated blank was quenched between two water-cooled plates at a defined contact pressure. During the test, the temperatures of the blank and of both contact plates were recorded. On the basis of the measured parameters, the heat transfer coefficient was calculated in dependence on the contact conditions using an analytical method according to Newton's cooling law.

$$T(t) = (T_0 - T_\infty)e^{(-h(A/c_p\rho V)t)} + T_\infty \quad (5)$$

A: contact surface, c_p: heat capacity, h: heat transfer coefficient, V: volume, t: time, T_0: initial temperature, T_∞: environmental temperature, ρ: density

The evaluation of the heat transfer coefficient h as a function of the increasing contact pressure shows the significant influence of the applied load on the heat exchange between workpiece and die (Fig. 10). Increasing the contact pressure leads to an increase of the heat transfer. This effect is related to the rise in the effective contact surface between the two contact partners through smoothing, in particular of the case in the Al–Si coated sheets. Consequently, more and more real metallic–metallic contact areas occur enforcing direct heat conductance effects, through which more thermal energy between the two contact bodies is transferred (Karbasian et al., 2008a,b).

6.2. Flow behavior

The flow behavior of steel 22MnB5 was characterized using a conductive hot tensile test by Merklein and Lechler (2006) to determine the material thermo-mechanical properties under process-relevant conditions (Fig. 11). This investigation showed

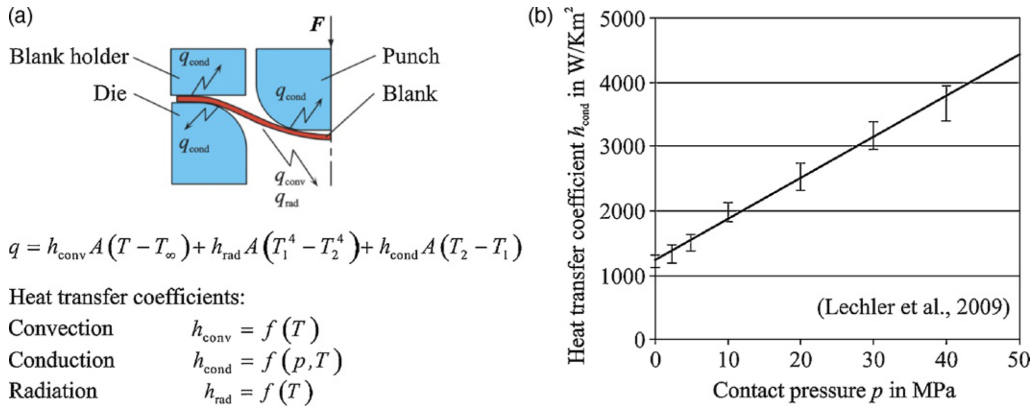

Fig. 10. Heat transfer coefficients in hot sheet forming.

that not only strain but also strain rate temperature and temperature rate have the greatest influence on the flow properties of 22MnB5 at elevated temperatures in the austenitic state.

Apart from the significant impact of the temperature and strain rate on the thermo-mechanical properties in the conductive tensile tests, the dependency of the temperature on the plastic anisotropy could be detected (Merklein and Lechler, 2008). At a temperature of about 800–850 °C, the sheet metal exhibits an almost isotropic plastic behavior. Because of austenitization, the influence of the anisotropy can be neglected (Merklein and Lechler, 2008).

6.3. Material models

For the thermo-mechanical forming processes, a large variety of semi-empirical as well as physically based models for the flow stress have been proposed. The existing models in Table 3, that have shown a good capability of representing the flow behavior of 22MnB5 in recent publications, are fitted to the experimental data by Hochholdinger et al. (2009) and Durrenberger et al. (2009). The experimental data for the determination of the flow stress are obtained by an upsetting test, which was conducted in a high-speed deformation dilatometer (Hochholdinger et al., 2009). The parameter estimation of some of the material models in Table 3 are not published in the cited references. But the other material data like those of Johnson–Cook and Norton–Hoff can be found in Åkerström (2006) and Lechler (2009).

Hochholdinger et al. (2009) have shown that the best fit of the experimental data can be achieved with the Tong–Wahlen model. Fig. 12a shows the failure in the saturation of the flow stress increases at higher values of the effective plastic strain in Norton–Hoff and the Nemat-Nasser model.

The values of the flow stress at relatively large strains represent the main disadvantage of the Johnson–Cook model in the work of Durrenberger et al. (2008, 2009) (Fig. 12b). The predictions of the Voce–Kocks relation are in good agreement with the experimental data, the model predicts an early saturation of the flow stress at a strain of about 0.06, while a slight strain-hardening is still observed in experiments. The Molinari–Ravichandran model has the capacity to reproduce history effects, such as rapid changes in strain rate or temperature history, by means of the evolution law of the internal parameter. However, for the material 22MnB5 analyzed in this study, the Molinari–Ravichandran model predicts an early saturation of the flow stress after a plastic strain of about 0.10. The predictions of the Ghost model are in good agreement with the experimental data of 22MnB5 up to a plastic strain of about 0.05.

A continuous model of the flow behavior, which includes and describes the phase transformation up to the end of the martensite evolution, is developed and implemented in a finite element simulation by Åkerström et al. (2007). The created model describes the thermo-mechanical material properties on the basis of the actual phase structure considering latent heat, volume change and transformation plasticity during phase transformation (Åkerström et al., 2005). The comparison of the material models with the experimental data has shown that the realistic modeling of the flow behavior of 22MnB5 in the austenite condition is possible.

6.4. Forming limit curve

The description of the material formability by sheet metal forming is traditionally achieved through the approach of forming limit curves FLC. This curve shows necking and fracture in the deformed sheet at different stress states on sheet samples from balanced

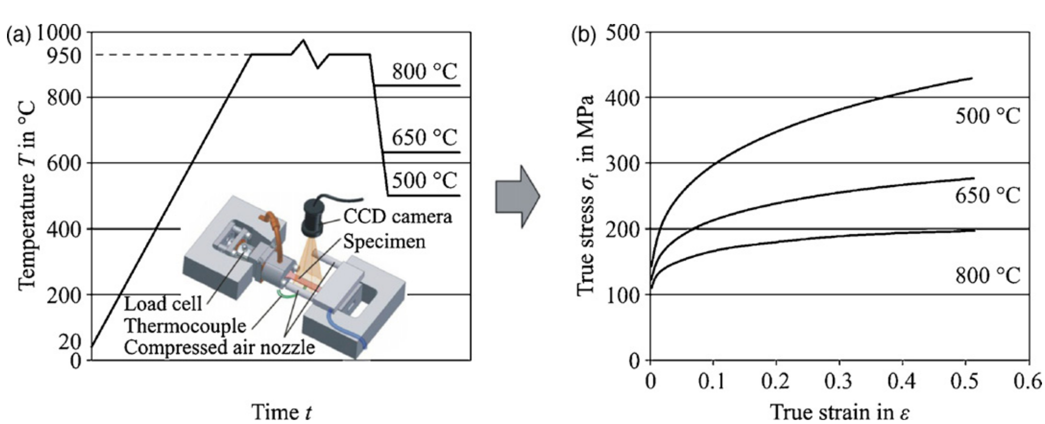

Fig. 11. (a) Experimental setup and (b) flow curves (Merklein and Lechler, 2006).

Table 3
Material models for 22MnB5.

Åkerström (2006)	Nemat-Nasser (1999)	$\sigma_f = \sigma_0 \left\{ 1 - \left[-\frac{kT}{G_0} \left(\ln \frac{\dot{\varepsilon}}{\dot{\varepsilon}_0} + \ln f(\varepsilon_p, T) \right) \right]^{1/q} \right\}^{1/p} f(\varepsilon_p, T) + \sigma_a^0 \varepsilon_p^n$ (6) $f(\varepsilon_p, T) = 1 + a_0 \left[1 - \left(\frac{T}{T_m} \right)^2 \right] \varepsilon_p^{1/2}$ σ_0: effective stress, k: Boltzmann constant p, q: shape of energy barrier, ε_0: reference strain, G_0: magnitude of activation energy, T: temperature
	Johnson and Cook (1983)	$\sigma_f = (A + B\varepsilon^n) \left[1 + C \ln \left(\frac{\dot{\varepsilon}}{\dot{\varepsilon}_0} \right) \right] \left[1 - \left(\frac{T - T_0}{T_f - T_0} \right)^m \right]$ with $T \geq T_0$ (7) A, B, C, n, m: coefficients of the model, $\dot{\varepsilon}_0$: reference strain rate, T: temperature, T_0: reference temperature, T: melting temperature
Hochholdinger et al. (2009)	Norton (1929) and Hoff (1954)	$\sigma_f = K(b + \varepsilon)^{n_0 \exp[-c_n(T-T_0)]} \dot{\varepsilon}^{m_0 \exp[c_m(T-T_0)]} \exp \left(\frac{\beta}{T} \right)$ (8) K, β, b, n_0, m_0, c_n, c_m: coefficients of the model, T: temperature, T_0: reference temperature
	Tong et al. (2005)	$\sigma_f = A \left[\dot{\varepsilon}^{m_1(T-T_0)} \exp \left(\frac{m_2 Q}{RT} \right) \right] \left[1 - \beta \exp \left(-N\varepsilon_p^n \right) \right]$ (9) A, m_1, m_2, N, β: constants of the model, R: gas constant, Q: activation energy, T: temperature, $\dot{\varepsilon}_p$: strain rate
Durrenberger et al. (2009)	Ghost (Bouaziz et al., 2004)	$\sigma = \left(\sigma_0 + M\alpha\mu b \sqrt{\rho} \right) \left(1 + \frac{kT}{b^3 \tau_{va}} arsh \left[\frac{\dot{\varepsilon}}{\dot{\varepsilon}_0} \exp \left(\frac{Q}{RT} \right) \right] \right)$ (10) M: Taylor factor, α: dislocation parameter, μ: shear modulus, b: Bürgers vector, ρ_0: dislocation density, k: Boltzmann constant, R: gas constant, σ_0: friction resistance, τ_{va}: shear stress, $\dot{\varepsilon}_0$: reference strain rate
	Molinari and Ravichandran (2005)	$\sigma_f = \hat{\sigma}_0 \left(\frac{\dot{\varepsilon}}{\dot{\varepsilon}_0} \right)^{1/m}$ with $\hat{\sigma}_0 = \hat{\sigma}(d) \left(\frac{\delta_0}{\delta} \right)$ (11) $\dot{\varepsilon}$: strain rate, $\dot{\varepsilon}_0$: reference strain rate, $\hat{\sigma}_0$: intrinsic resistance, m: instantaneous material rate sensitivity, d: grain size, T: temperature
	Voce–Kocks (1976)	$\sigma_f = \sigma_S + \left[(\sigma_0 - \sigma_S) \exp \left(-\frac{\varepsilon}{\varepsilon_r} \right) \right]$ (12) σ_s: saturation stress, σ_0: initial yield stress, ε_r: relaxation strain

biaxial to pure shear. However, when forming take places at elevated temperatures, the material formability is greatly influenced not only by the strain but also by temperature, strain rate, and microstructural evolution during deformation (Pellegrini et al., 2009).

Several tests have been developed and applied for this purpose, with the Marciniak and the Nakajima tests being the most commonly applied ones. In both tests, the sheet metal – in the metastable austenitic phase – undergoes thermo-mechanical treatments, that are carried out at different temperatures and follow different paths of strain and strain rate until the onset of necking and fracture occurs (Bariani et al., 2008). The main difference between these tests is the shape of the punch, which is either hemispherical or flat (Dahan et al., 2007).

Forming limit curves of the material 22MnB5 were measured in the Nakajima tests at elevated temperatures in different studies. Here, for the determination of the temperature-dependent forming limit curves, the traditional test equipment has to be modified. Therefore, special heating cartridges have to be introduced in the punch, the die, and the blank holder to control the temperature of the setup.

Pellegrini et al. (2009) have shown that the thermally induced improvement of the material and higher values of the slip systems of austenite in comparison to the initial ferrite-pearlite microstructure are the cause of the evolution of the mechanical properties during hot stamping (Fig. 13). The main reasons for the scattering of the analyzed results are the different procedure and the evaluation tests at elevated temperatures. The heating method by Lechler (2009) ensures a uniform distribution of the blank temperature during the heating phase in the furnace, but implies a more difficult control of the temperature during cooling due to the manual transfer to the press. The induction heating of Pellegrini et al. (2009) leads to a less uniform distribution of the temperature but also to a good cooling control.

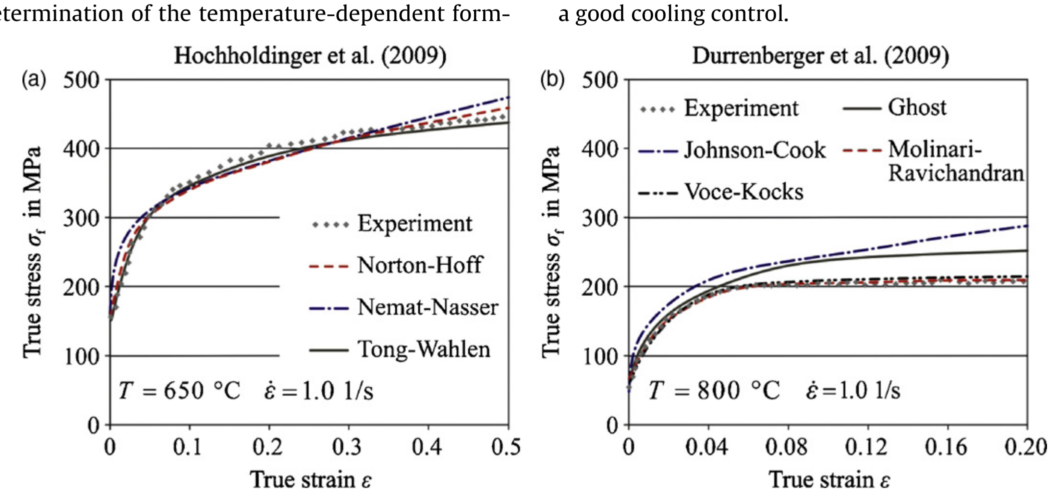

Fig. 12. Flow curves of different models for 22MnB5 and the experiments.

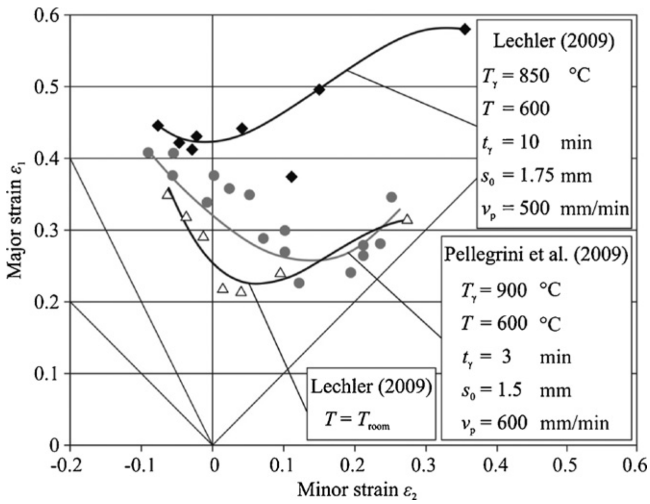

Fig. 13. Forming limit curves of 22MnB5.

Similar to cited works of Pellegrini et al. (2009) and Lechler (2009), Chastel et al. (2008) have shown that the higher the initial blank temperature or the sheet thickness, the higher the critical strain in plane strain.

In the existing works, heating and cooling of the blank are accomplished by different methods. On the one hand, in the work by Lechler (2009), the heating method ensures a uniform temperature distribution on the blank during the heating phase in the furnace. However, this implies a more difficult control of the temperature during cooling due to the manual transfer to the press. On the other hand, the induction heating used in the work by Bariani et al. (2008) leads to a less uniform distribution of temperature but allows a good cooling control, ensuring very high cooling rates. Therefore, the difficulty in carrying out tests under real isothermal conditions at high enough cooling rates to ensure the avoidance of any phase transformation is evident. The issue of evaluating sheet metal formability at elevated temperatures can be accomplished through an alternative approach, based on the application of a proper failure criterion that can be developed as a function of strain, strain rate, temperature, and microstructural evolution (Pellegrini et al., 2009).

6.5. Friction coefficient

The friction characteristics of the coated material used in hot stamping can be evaluated by different test methods (Fig. 14). The testing methods vary in the contact condition between the sheet and the tool, which is important for the determination of the friction coefficient and must be similar to hot stamping conditions.

An experimental–analytical–numerical evaluation method was used by Stöhr et al. (2008) to determine the friction coefficient under process-relevant conditions. Here, the cup deep drawing test (Fig. 14a), following the time–temperature profile of the hot stamping process, acted as experimental basis. To reveal different thermal conduction rates during the experiments with the objective to investigate the impact of the temperature on the tribological conduction rates, the temperature of the tool was varied. In this work, the friction values determined for Al–Si coated 22MnB5 specimens were calculated by Siebel's approach (Siebel and Beisswänger, 1955). The results (Fig. 15) show a significant decrease of the friction coefficient with rising temperature, with the values ranging from 0.6 to 0.3 (Stöhr et al., 2008).

The pin-on-disc test (Fig. 14b) was performed by Ghiotti et al. (2009a,b) and by Hardell and Prakash (2008) to investigate the influence of the process parameters (i.e. temperature, pressure, sliding velocity and roughness) on the friction at the interface between the sheet metal blank and the dies. The analysis has shown that the interaction between the temperature and the pressure is the most relevant one for the friction coefficient in hot stamping. Both studies have shown that the friction value of the interface decreases with increasing temperature and normal pressure. This fact may be explained by the formation of the intermetallic Fe–Al, which is responsible for the friction reduction when increasing normal pressure is applied (Ghiotti et al., 2009a,b). The contact condition between the blank and the tool in the pin-on-disc method is different from the contact condition in sheet metal forming. Therefore, the determined values of up to 0.8 (Fig. 15) using this method are not suitable for the application in sheet metal forming under the corresponding surface contact condition.

Another method for the determination of the friction is the drawing test (Fig. 14c), which was carried out by Dessain et al. (2008). The heated sheet is drawn through the convex contact area of the tool with a simultaneous measurement of the forces in different directions. The friction coefficient is calculated from the measured forces according to Pawelski (1964). A comparison of the results for the friction coefficient at a constant pressure of 10 MPa and a constant austenitization time in the furnace of 390 s reveals that different temperature values have only a small influence on the frictional behavior of the tribological system (Fig. 15). The same is true for a higher surface pressure value of 25 MPa (Dessain et al., 2008).

The last method used to evaluate the friction coefficient is strip drawing (Fig. 14d), applied by Yanagida and Azushima (2009). The testing machine consists of a furnace and a drawing device with an integrated blank holder. The friction coefficient is calculated from the blank holder force and the tension force. In contrast to other cited investigations, the calculated friction coefficient of 0.5 up to 0.6 increases with increasing temperature at a constant pressure of

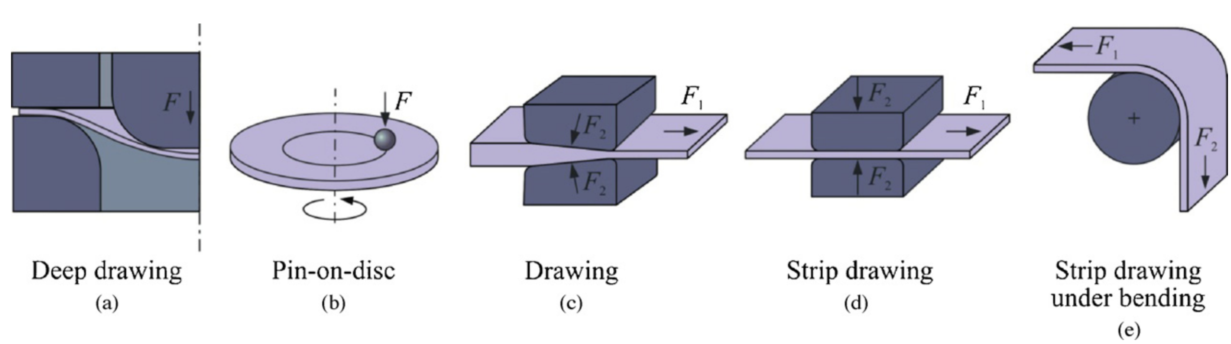

Fig. 14. Principle of the test methods for the evaluation of friction characteristics.

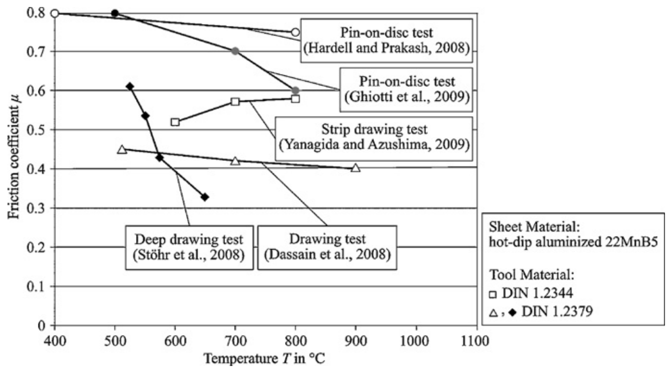

Fig. 15. Friction coefficient against temperature.

10 MPa (Fig. 15). The variation of the contact pressure between 7 and 14 MPa has shown that the friction coefficient is independent of the contact pressure within this range (Yanagida and Azushima, 2009).

The results of the different investigations on the friction coefficient of Al–Si coated 22MnB5 (Fig. 15) show that the contact condition during the test has a great influence on the calculated values. In comparison to the real hot stamping process, the contact conditions are similar to those in deep drawing (Fig. 14a) and strip drawing under bending (Fig. 14e). The strip drawing under bending has not been used for the determination of the friction coefficient.

7. Final properties

The martensite evolution during quenching causes an increased tensile strength of up to 1500 MPa, which is verified in different works using tensile tests (Naderi, 2007) and hardness measurements (Åkerström, 2006). The subsequent microstructure investigations have shown that the full martensite transformation is the precondition for the increased mechanical strength of the material. Due to the effect of the cooling rate and the phase transformation, the final mechanical properties are dependent on the process control.

In a continuous cooling process, cooling rate and hardness are the relevant parameters. In a practical approach, Erhardt and Böke (2008) used the cooling gradients, calculated in the hot forming simulation, to determine a value of hardness and other mechanical characteristics of the part. The mechanical properties depend on the thermal and forming history of the part.

The flow curves of 22MnB5 at different temperatures and strain rates show the strong influence of these process parameters on the flow behavior of the material. Although temperature and strain rate are varied along the part surface and process in the course of the time, the studies of Yanagimoto and Oyamada (2007) and Kusumi et al. (2009) have shown the high shape accuracy of the hot stamped parts with minimal springback.

For the description of the thermo-mechanical phenomena during hot stamping and their background, the analysis of residual stress is required. In further investigations, the analysis of the stress fractions due to thermo mechanical and microstructural procedures can be the dominant process parameters with regard to the part properties. This knowledge is also essential for the distortion-free manufacturing of hot stamped parts with tailored properties.

7.1. Corrosion

The same cathodic protection of cold formed parts is desirable for hot stamped parts. The surface of the Fe–Al alloy phase of hot-dip aluminized sheets after the heat treatment is rough, and thanks to an anchoring effect of the surface, its paintability is good without chemical treatment. The Fe–Al alloy phase exhibits a better corrosion resistance than a steel sheet without surface treatment and an almost equivalent corrosion resistance to that of a galvannealed steel sheet (Suehiro et al., 2003). It must be pointed out that the Al–Si coating does not provide cathodic protection like zinc but a high barrier protection.

For the corrosion tests with x-tec coated blanks, it has been clarified that the corrosion does not come from the steel basic material and is not produced by iron diffused into the coating during the annealing process (Goedicke et al., 2008). To ensure weldability and paint adherence, the x-tec® coating has to be removed after press hardening by shot blasing (Paar et al., 2008).

The measured protection against perforation corrosion of a phs-ultraform® (Zn–Fe coated) blank shows that the Zn–Fe coating performs significantly better than conventional zinc coatings. This is due to a slightly higher electrochemical potential in this coating and more stable corrosion products (Faderl et al., 2008). Also in terms of paint delamination, the discussed Zn–Fe coating is superior to conventional galvanized coatings as long as the surface is properly conditioned. Red-colored corrosion products (yellow rust) may occur as a result of the iron content in the protective coating, analogously to galvannealed coatings. The cross-section of the corroded sample clearly demonstrates that the base steel has not been attacked for a very long time (Faderl et al., 2009).

The subject of the current investigations is the continuous improvement of established coatings and the development of new or modified metallic coatings with an active corrosion protection suitable for the direct process. One of the goals is to combine the high thermal stability of Al–Si coatings with the cathodic protection of Zn coatings for the direct and indirect process. Another goal is to avoid intercrystalline cracks during hot stamping by using prealloyed zinc coatings (Paar et al., 2008).

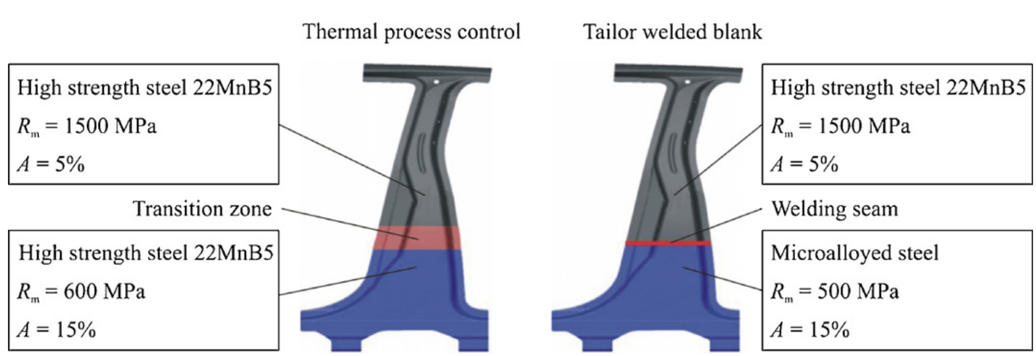

Fig. 16. B-pillar with tailored properties (Erhardt and Böke, 2008).

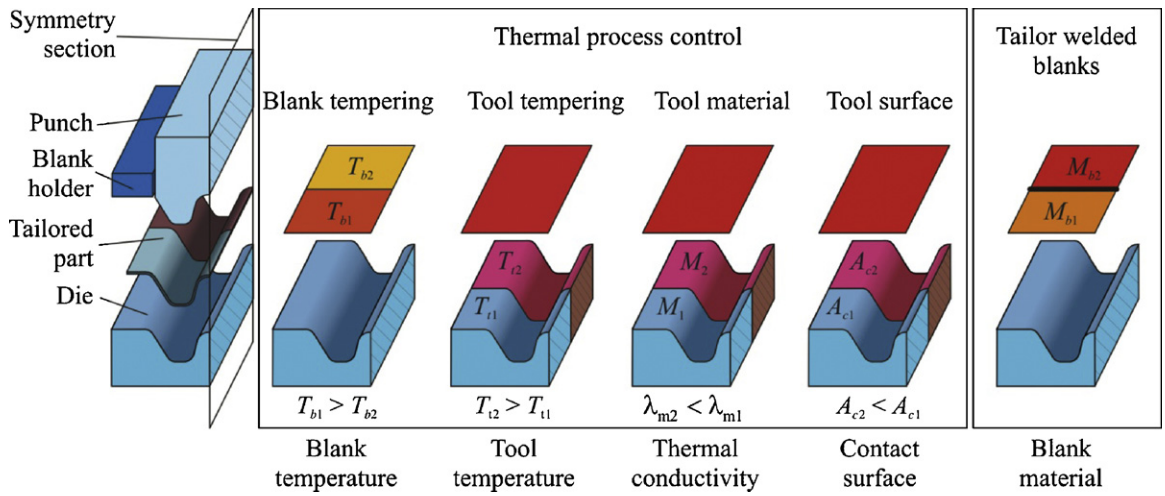

Fig. 17. Different methods for hot stamping of the parts with tailored properties.

8. Subsequent processing

Because of the special mechanical properties, the subsequent processing of the hot stamped parts requires a process analysis and an adapted process window in regard to the relevant parameters. In the following, cutting and joining as the most important subsequent processing of hot stamped parts will be described and their applicability in series production will be evaluated.

8.1. *Cutting*

Similar to conventional sheet metal forming, cutting or piercing are the next stage in the hot stamping process chain after forming and, if necessary, shot blasting. The different methods used for cutting hot stamped parts are reviewed.

8.1.1. *Laser cutting*

Because of the high strength of the material after hot stamping, laser cutting is the most commonly used method for cutting hot stamped parts. Due to the contactless trimming laser, cutting does not cause any tool wear or any failure on the cutting edge in contrast to other cutting methods. Another advantage of using laser cutting is the fact that there are nearly no limits with regard to the shape of the parts to be trimmed. The achievable tolerances are influenced by the stiffness of the laser machine and the holding fixture of the part. The laser cutting time depends on the part geometry and the movement of the laser machine (Kolleck et al., 2009a,b).

8.1.2. *Hard cutting*

The achieved high strength of press-hardened parts causes severe blanking tool wear and sometimes early tool failure with conventional mechanical blanking methods. So et al. (2009) have shown that in the blanking process, the quality of the sheared surface and the dimension precision are influenced by certain process parameters, such as punch speeds, blanking angles, punch-die clearances, tool cutting edge geometries, and the mechanical properties of the material. In this study, no influence of the punch speed on the sheared geometries and the blanking forces are observed. For all tested blanking angles, the rollover increases with increasing punch-die clearance. Furthermore, a noticeable result is found in the fact that the ratio of the burnish depth increases as the clearance increases until the burr forms, but decreases again with increasing clearance after burr formation (So et al., 2009).

Another investigation on hard cutting by Picas et al. (2008) shows that the high hardness of the punch induces low wear of the cutting edge, but it becomes strongly sensitive to high loads during its application since considerable microfractures occur along the cutting edge. In the high-toughness punch, a slight reduction of wear resistance is produced in the cutting edge, but this is compensated by a high toughness and fatigue resistance. Therefore, an optimal toughness-hardness compromise must be found to improve the mechanical behavior of tools, especially in cutting of press-hardened parts (Picas et al., 2008).

8.1.3. *Warm cutting*

Another alternative for cutting hot stamped parts is cutting of parts during quenching at elevated temperatures. The advantages of warm cutting are a reduced cutting force and an optimized cutting edge through a short process chain.

The latest innovative procedure is the selective heat treatment of the parts during quenching. In order to avoid martensite transformation, the cooling rate in the cutting areas must be reduced. Locally differentiated heat treatments in the hot stamped components can be performed by means of differentiated heat transfer rates designed for improvement of posterior cutting, and one of the preferred ways to achieve this is trough the employment of tool materials with different thermal conductivities (Maikranz-Valentin et al., 2008).

The most cost-effective cutting method is pre-developed blanking. This method requires a certain blank design to achieve the desired part outline after forming (Kolleck et al., 2009a,b). The tol-

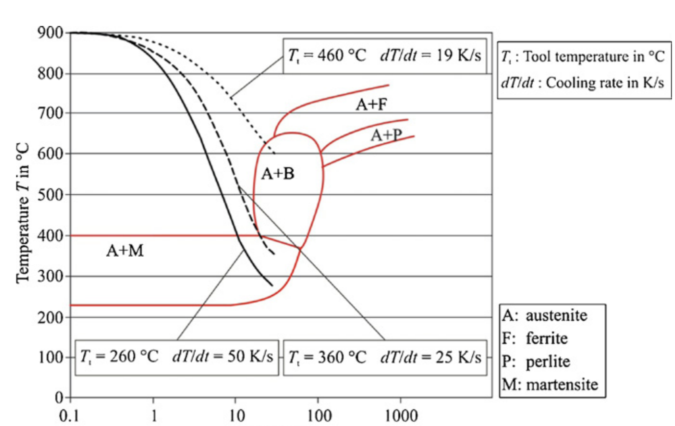

Fig. 18. Cooling curves for different tool temperatures (Ghiotti et al., 2009a,b).

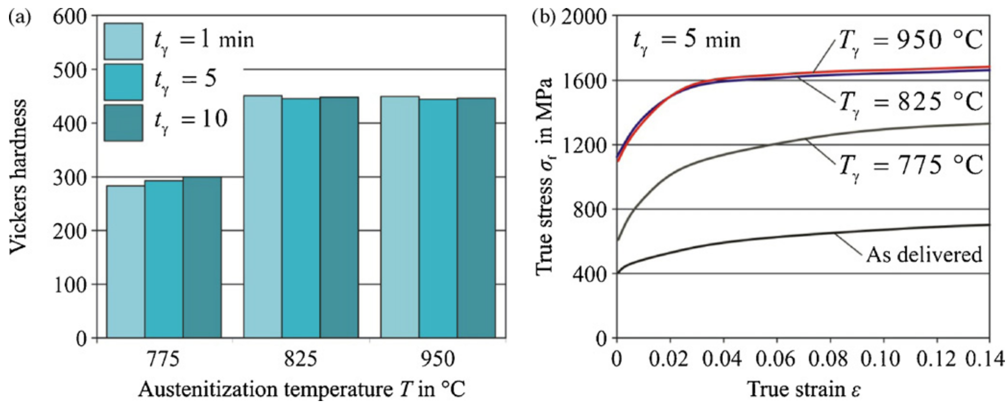

Fig. 19. Mechanical properties at different austenitization temperatures (Stöhr et al., 2009).

erances that can be achieved are smaller than with cutting after hot forming.

8.2. Joining

Because of the low formability, the joining by forming methods cannot be applied for joining hot stamped parts. Therefore, weldability of the hot stamped parts is the precondition for the application of the parts in practice. The coating layer and its chemical composition can cause failures during welding. In the following, the investigations on resistance spot welding, laser and gas metal arc welding of the material 22MnB5 with different coatings are reviewed.

The aluminum plating layer of the product is transformed during heating before being press-formed into a Fe–Al alloy phase having a high melting point, and, thanks to this, the spot-weldability of the product is not affected by the presence of coating layers (Suehiro et al., 2003).

The first generation scale protection, e.g. x-tec®, is not spot-weldable and must therefore be removed by sandblasting from the press-hardened parts before further processing. The reason for this behavior is that the electric resistance of the anti-scaling coating after the hot stamping process is too high to permit a sufficient flow of welding current. The test of second and third generation x-tec® anti scaling coatings by the integration of magnesium particles has shown the suitability of the coatings for resistance spot welding (Goedicke et al., 2008). Resistance spot welding (RSW) of x-tec® coated blanks has shown that the applied atmosphere inside the furnace while heating the blanks has a great influence on the spot-weldability. The O_2 content was found to be the main driver here. Heating in air causes the formation of oxide layers so that spot welding cannot be applied. Applying a nitrogen atmosphere leads to very low oxide percentages inside the coated layer after heating and forming, and thus supports spot welding (Braun and Fritzsche, 2009).

For Zn–Fe coatings, the best resistance spot welding results are produced with the double-pulse technology in combination with a DC source (Faderl et al., 2009). The other methods of joining are also possible, such as SG welding, SG brazing, laser and stud welding (Faderl et al., 2009).

For laser and gas metal arc welding, the cross-sections of the joints of the tested combinations show that the x-tec® coating had no influence on the welding behavior. No pores or other defects were detected inside the joints with and without overlap. This coating will flexibly work also with different substrates, e.g. H430LA for manufacturing tailor welded blanks (Braun and Fritzsche, 2009). In order to avoid the diffusion of Al and Si into the weld seam, when the hot-dip aluminized sheets are used, the coated layer must be removed about 2 mm along the weld seam.

9. Hot stamped parts with tailored properties

The fully martensitic transformation during hot stamping of the parts leads to a tensile strength of up to 1500 MPa and a low elon-

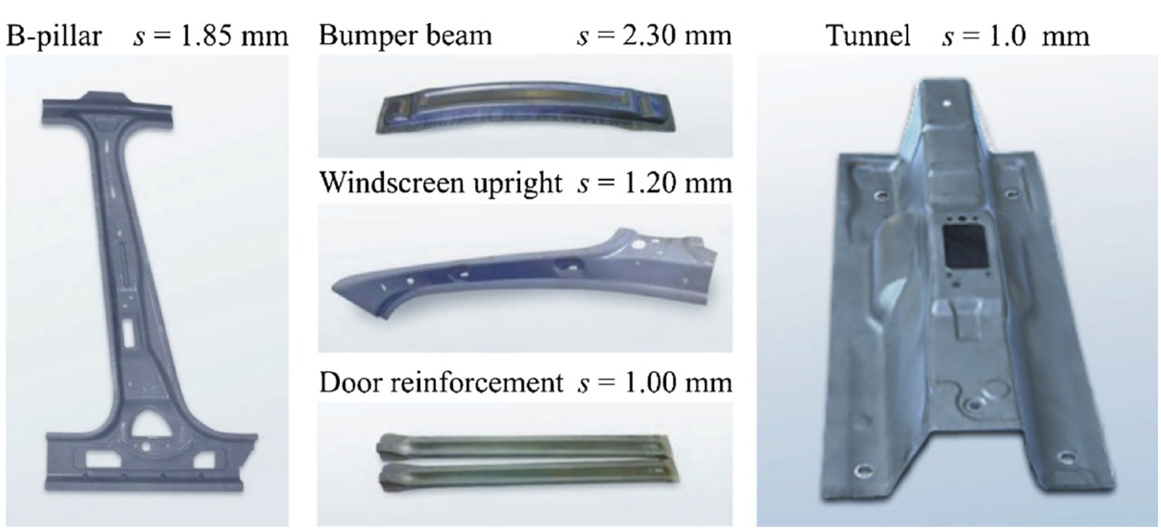

Fig. 20. Hot stamped parts in automotive industry (N. N., 2008).

gation of about 5%. But an improved crash performance of a vehicle structural component (such as a B-pillar) can be achieved by introducing regions which have an increased elongation for improved energy absorption. The B-pillars shown in Fig. 16 have an excellent intrusion control in the upper section and a high energy absorption in the lower section.

The manufacturing of a single part with tailored properties can be carried out using different process control strategies or using tailor welded blanks (Fig. 17).

Alternatively, the thermal process can be influenced by reducing the cooling rate below the specific 27 K/s to avoid a fully martensitic microstructure in defined areas of the component during the forming process, or by reducing the annealing temperature below the material-specific Ac_3 temperature, which leads to an incomplete austenitization. Both methods implicate a lower strength and therefore a higher ductility. The other areas of the component are quenched, following the commonly known press hardening time–temperature profile (Stöhr et al., 2009).

9.1. Tool tempering

The reduction of the quench rate can be achieved by increasing the temperature of the die, which will reduce the heat transfer by conduction between the blank and the die surface. It is possible to heat and cool different regions of a die, which will generate localized regions of high strength (fully martensitic) and other regions of higher ductility (mixture of daughter phases). Experimental and numerical studies by Lenze et al. (2008a,b) indicate that it is possible to create a part with areas of very high strength for intrusion protection, and others regions with increased ductility and energy absorption. The selected tool tempering influences the cooling rate during quenching and the final phases of the material. Therefore, the material properties of the parts can be selectively adjusted by means of the different tool temperatures (Fig. 18).

9.2. Tool material

The locally differentiated heat treatment within a tool system can be achieved by the application of tool materials with different thermal conductivities. A modular tool system consists of tool sequences made of tool steels developed by Casas et al. (2008) with thermal conductivities from 7 W/mK up to 66 W/mK. In this way, the heat transfer can be controlled along the part surfaces. Because of different thermal boundary conditions within the system, the tool sequences achieve the thermal steady state by different strokes. This thermal phenomenon and its effect on the part properties must be investigated in further studies.

9.3. Tool surface

The heat transfer during quenching is affected by the contact condition between the part and the tool. The numerical investigation by George et al. (2009) on the thermal behavior of tool systems with integrated partial contact gaps has shown that in the regions of the air gaps, the cooling rates of the part can be reduced below the critical rate of the martensite transformation. A disadvantage of this method is the free forming of the part in the contact gap area, which can decrease the shape accuracy of the part. Another method for the local reduction of heat transfer can be surface structuring. The structured surface reduces the effective contact area. The investigation of the effect of structured surfaces on the heat transfer coefficient can be the focus of an innovative manufacturing of hot stamped parts with tailored properties.

9.4. Blank tempering

Heating above Ac_3 can be done locally in the zones of the blank where a martensitic structure is to be achieved. In this way, the complete thermal cycle above austenitization would be applied only in these zones, whereas all the others zones would retain the original ferritic-pearlitic structure. Ghiotti et al. (2009a,b) indicate that the use of a furnace with areas kept at different temperatures and the employment of resistance heating are two approaches that appear to be the most suitable ones for this application. However, it has to be taken into account that the different material behaviors in the two areas influence the forming process accordingly. The formability may be reduced in the section with a lower temperature and, additionally, springback may occur (Erhardt and Böke, 2008). The investigation on the thermo-mechanical properties at different annealing temperatures by Stöhr et al. (2009) has shown that for the applicability of lower annealing temperatures to achieve a lower ductility profile for components with tailored properties, a temperature lower than 825 °C has to be chosen to assure a significantly lower strength and hardness than that of commonly hot stamped sheet metal (Fig. 19).

9.5. Tailor welded blanks

Forming of tailor welded blanks or profiles at room temperature is already the state of the art in various applications in the automotive industry. Similar to this, the application of tailor welded blanks in hot stamping allows the manufacturing of parts with tailored properties. Here, the blanks made of heat-treatable and non-heat-treatable steel grades will be hot stamped. Because of the martensite evolution in the heat-treatable steel, the final part strength increases contrary to that of the non-heat-treatable steel. The blanks are laser welded. Before this, the coating of the weld zone must be removed. The position of the weld seam and its limited formability during hot stamping are further important aspects to be considered in the process design of tailor welded blanks.

10. Applications

The combination of forming and hardening makes 22MnB5 steel an ideal solution for the construction of structural elements and safety-relevant components in the automotive industry, in particular in view of the implementation of penetration protection in the areas of the passenger cabin or motor (N. N., 2008). Some automotive applications of hot stamping are A-pillars, B-pillars, side impact protections, sills, frame components, bumpers, bumper mounts, door pillar reinforcements, roof frames, tunnels, rear and front end cross members (Fig. 20). The sheet thickness in these parts varies between 1.0 and 2.5 mm.

11. Conclusion

In this review, the recent investigations on hot stamping of high strength steels are summarized with the objective to evaluate the different research results. This general survey has revealed the existing gaps in the knowledge by describing specific phenomena of hot stamping. Furthermore, some innovative procedures for further developments in the field of hot stamping are identified.

The application and subsequent processing of the hot stamped part depend on an efficient cutting system as well as the part weldability and surface texture. In order to avoid the oxide scale formation during austenitization, most sheet metals used for hot stamping are pre-coated. The objective of current developments is to obtain a universal coating material for the direct and indirect hot stamping process with additional cathodic protection.

The cycle time for press-hardened parts is mainly dependent on the die closing time and the furnace residence time required to austenitize the material and, as to the coating, to achieve the required through-alloying. With regard to die closing time, optimizing the cooling of the die or the tool steels used could provide a reduction in cycle time. A reduction in furnace residence time can only be achieved by faster heating concepts, like conductive or inductive heating. Therefore, the alternative heating systems (conduction and induction heating) exhibit a great potential for the future.

Hot stamping is a thermo-mechanical forming process with intended phase transformation. Consequently, a realistic FE model for the process simulation must consider the interaction between the mechanical, thermal, and microstructural fields. This can only be achieved by means of process characteristics, like e.g. the heat transfer coefficient, the material flow behavior and phase transformation under process-relevant conditions.

The comparison of the material models with the experimental data has shown that a realistic modeling of the flow behavior of 22MnB5 in the austenitic condition is possible. The continuous model of the flow behavior must consider the thermo-mechanical material properties on the basis of the actual phase structure considering latent heat, volume change and transformation plasticity up to the end of the martensite evolution. Furthermore, the sheet metal formability at elevated temperatures can be evaluated through the application of an appropriate failure criterion, that can be developed as a function of strain, strain rate, temperature, and microstructural evolution.

The flow curves of 22MnB5 at different temperatures and strain rates show the strong influence of these process parameters on the flow behavior of the material. Several studies have shown the high shape accuracy of the hot stamped parts with minimal springback within an optimized process window of conventional hot stamping. However, for the distortion-free manufacturing of hot stamped parts with tailored properties it is also essential to investigate the influence of different phase transformation procedures within the tailored parts on the geometrical and mechanical part properties.

This thorough survey of the existing works on novel process configurations has shown the great potential for the application of high strength steels using hot stamping. Furthermore, basic knowledge of the physical phenomena during hot stamping is the precondition for an optimal process design.

References

Åkerström, P., 2006. Modeling and simulation of hot stamping. Doctoral Theses, Luleå University of Technology, Sweden.

Åkerström, P., Wikman, B., Oldenburg, M., 2005. Material parameter estimation for boron steel from simultaneous cooling and compression experiments. Modelling and Simulation in Materials Science and Engineering 13, 1291–1308.

Åkerström, P., Bergman, G., Oldenburg, M., 2007. Numerical implementation of a constitutive model for simulation of hot stamping. Materials Science and Engineering 15, 105–119.

Aspacher, J., 2008. Forming hardening concepts. In: 1st International Conference on Hot Sheet Metal Forming of High-Performance Steel, Kassel, Germany, pp. 77–81.

Austerhoff, N., Rostek, W., 2002. Hot Stamping und Wärmebehandlung von höchstfesten Stählen am Beispiel von Karosserie- und Fahrwerksbauteilen. In: Stahl-Spaceframes contra Schalenbauweise, Tagungsband zur 5, Europäischen Karosserie-Leichtbau-Konferenz, Bad Neuheim, Germany, pp. 1–10.

Bariani, P.F., Bruschi, S., Ghiotti, A., Tureta, A., 2008. Testing formability in the hot stamping of HSS. CIRP Annals—Manufacturing Technology 57, 265–268.

Behrens, B.A., Hübner, S., Demir, M., 2008. Conductive heating system for hot sheet metal forming. In: 1st International Conference on Hot Sheet Metal Forming of High-Performance Steel, Kassel, Germany, pp. 63–68.

Bergman, G., 1999. Modeling and Simultaneous forming and quenching. Doctoral Theses, Luleå University of Technology, Schweden.

Bergman, G., Oldenburg, M., 2004. A finite element model for thermo-mechanical analysis of sheet-metal forming. International Journal for Numerical Methods in Engineering 59, 1167–1186.

Berglund, G., 2008. The history of hardening of boron steel in northern Sweden. In: 1st International Conference on Hot Sheet Metal Forming of High-Performance Steel, Kassel, Germany, pp. 175–177.

Borsetto, F., Ghiotti, A., Bruschi, S., 2009. Investigation of the high strength steel Al–Si coating during hot stamping operations. Key Engineering Materials 410–411, 289–296.

Bouaziz, O., Quidort, D., Feuillu, D., 2004. An unified description of non-steady state deformation for steels in the austenitic temperature range. In: 41st Thermomech. Proc. of Steels, Belgium.

Braun, M., Fritzsche, Ch., 2009. Joining of hot-formed steel. In: 2nd International Conference on Hot Sheet Metal Forming of High-Performance Steel, Luleå, Sweden, pp. 313–322.

Casas, B., Latre, D., Rodriguez, N., Valls, I., 2008. Tailor made tool materials for the present and upcoming tooling solutions in hot sheet metal forming. In: 1st International Conference on Hot Sheet Metal Forming of High-Performance Steel, Kassel, Germany, pp. 23–35.

Chastel, Y., Dahan, Y., Massoni, E., Duroux, P., Wilsius, J., Hein, P., 2008. Formability of quenchable steels in hot stamping. In: The 9th International Conference on Technology of Plasticity, ICTP, Gyeongiu, Korea, pp. 678–683.

Dahan, Y., Chastel, Y., Duroux, P., Wilsius, J., Hein, P., Massoni, E., 2007. Procedure for the experimental limit curve for USIBOR 1500 P. International Deep Drawing Research Group IDDRG, Győr, Hungary, pp. 125–132.

Dessain, Ch., Hein, P., Wilsius, J., Penazzi, L., Boher, Ch., Weikert, J., 2008. Experimental investigation of friction and wear in hot stamping of usibor 1500P. In: 1st International Conference on Hot Sheet Metal Forming of High-Performance Steel, Kassel, Germany, pp. 217–227.

Durrenberger, L., Saeed-Akbari, A., Bleck, W., 2008. The effects of non-isothermal deformation on martensitc transformation in 22MnB5 steel. Materials Science and Engineering A 478, 445–455.

Durrenberger, L., Wilsius, J., Hein, P., 2009. Impact of the constitutive model on the hot-forming numerical predictions of usibor 1500P. In: 2nd International Conference on Hot Sheet Metal Forming of High-Performance Steel, Luleå, Sweden, pp. 51–58.

Erhardt, R., Böke, J., 2008. Industrial application of hot forming press simulation. In: 1st International Conference on Hot Sheet Metal Forming of High-Performance Steel, Kassel, Germany, pp. 83–88.

Faderl, J., Manzenreiter, T., Radlmayr, M., 2008. Press hardening of hot-dip galvanized 22MnB5: a stable and reproducible process. In: 1st International Conference on Hot Sheet Metal Forming of High-Performance Steel, Kassel, Germany, pp. 199–205.

Faderl, J., Kolnberger, S., Kurz, T., Luckeneder, G., Martenreiter, T., Rosner, M., 2009. phs-ultraform®—continuous galvanizing meets press-hardening. In: 2nd International Conference on Hot Sheet Metal Forming of High-Performance Steel, Luleå, Sweden, pp. 283–292.

Forstner, K., Strobich, S., Buchmayr, B., 2007. Heat transfer during press hardening. International Deep Drawing Research Group IDDRG, Győr, Hungary, 609–613.

Freieck, U., 2007. In zwei Wochen zum Serienwerkzeug. Blech 2, 46–47.

Garcia Aranda, L., Chastel, Y., Fernández Pascual, J., Dal Negro, T., 2002. Experiments and simulation of hot stamping of quenchable steels. Advanced Technology of Plasticity 2, 1135–1140.

George, R., Bardelcik, A., Worswick, M., 2009. Localized die temperature control for tailored properties in hot forming of boron steels—numerical study. IDDRG, Golden, CO, USA, 131–139.

Ghiotti, A., Borsetto, F., Bruschi, S., 2009a. Investigation of the high strength steel Al–Si coating during hot stamping operations. Key Engineering Materials 410–411, 289–296.

Ghiotti, A., Pellegrini, D., Bruschi, S., 2009. Feasibility of producing tailored microstructures in hot stamped sheet components. IDDRG, Golden, CO, USA, 941–950.

Ghosh, A., Kikuchi, N., 1988. Finite element formulation for the simulation of hot sheet metal forming processes. International Journal of Engineering Science 26 (2), 143–161.

Goedicke, S., Sepeur, S., Frenzer, G., Breyer, Ch., 2008. Wet chemical coating materials for hot sheet forming—anti scaling and corrosion protection. In: 1st International Conference on Hot Sheet Metal Forming of High-Performance Steel, Kassel, Germany, pp. 37–44.

Greenwood, G.W., Johnson, R.H., 1965. The deformation of metals under small stresses during phase transformations. Proceedings of Royal Society 283, 405–422.

Hardell, J., Prakash, B., 2008. High temperature friction and wear behavior of different tool steels during sliding against Al–Si-coated high strength steel. Tribology International 41 (7), 663–671.

Hein, P., 2005. A global approach of the finite element simulation of hot stamping. Advanced Materials Research 6–7, 763–770.

Hochholdinger, B., Grass, H., Lipp, A., Hora, P., 2009. Modeling and determination of flow curves for the simulation of hot forming. International Deep Drawing Research Group IDDRG, Golden, CO, USA, 659–669.

Hoff, N.J., 1954. Approximate analysis of structures in the presence of moderately large creep deformations. Q. Appl. Math. 12, 49–55.

Hoff, C., 2007. Untersuchung der Prozesseinflussgrößen beim Presshärten des höchstfesten Vergütungsstahls 22MnB5. Dr.-Ing. Dissertation, LFT, University of Erlangen-Nuremberg.

Hoffmann, H., So, H., Steinbeiss, H., 2007. Design of hot stamping tools with cooling system. CIRP Annals—Manufacturing Technology 56, 269–272.

Jeswiet, J., Geiger, M., Engel, U., Kleiner, M., Schikorra, M., Duflou, J., Neugebauer, R., Bariani, P., Bruschi, S., 2008. Metal forming progress since 2000. CIRP Journal of Manufacturing Technology 1, 2–17.

Johnson, G.R., Cook, W.H., 1983. A constitutive model and data for metals subjected to large strains, high strain-rates and high temperature. In: The 7th Symposium on Ballistic, pp. 541–547.

Karbasian, H., Brosius, A., Tekkaya, A.E., Lechler, J., Merklein, M., 2008a. Numerical process design of hot stamping processes based on verified thermo-mechanical characteristics. In: Materials Science and Technology (MS&T), Pittsburgh, Pennsylvania, pp. 1733–1743.

Karbasian, H., Klimmek, Ch., Brosius, A., Tekkaya, A.E., 2008b. Identification of thermo-mechanical interaction during hot stamping by means of design of experiments for numerical process design. In: Numisheet, Interlaken, Switzerland, pp. 575–579.

Kocks, U.F., 1976. Laws for strain-hardening and low-temperature creep. Journal of Engineering Materials and Technology 98, 76–85.

Koistinen, D.P., Marburger, R.E., 1959. A general equation prescribing the extent of the austenite-martensite tansformation in pure iron-carbon alloys and plain carbon steels. Acta Metallurgica 7, 59–60.

Kolleck, R., Veit, R., Hofmann, H., Lenze, F.J., 2008. Alternative heating concepts for hot sheet metal forming. In: 1st International Conference on Hot Sheet Metal Forming of High-Performance Steel, Kassel, Germany, pp. 239–246.

Kolleck, R., Aspacher, J., Veit, R., 2009a. Efficienty of hot forming processes. In: 2nd International Conference on Hot Sheet Metal Forming of High-Performance Steel, Luleå, Sweden, pp. 173–179.

Kolleck, R., Veit, R., Merklein, M., Lechler, J., Geiger, M., 2009b. Investigation on induction heating for hot stamping of boron alloyed steels. CIRP Annals—Manufacturing Technology 58, 275–278.

Kuhn, D., Kolleck, R., 2006. Warmumformung – den höheren Festigkeiten folgend. MM das IndustrieMagazin 17, 86–87.

Kusumi, K., Yamamoro, S., Takeshita, T., Abe, M., 2009. The effect of martensitic transformation on the spring-back behavior of the hot stamping. In: 2nd International Conference on Hot Sheet Metal Forming of High-Performance Steel, Luleå, Sweden, pp. 97–104.

Leblond, L.B., Devaux, J., Devaux, J.C., 1989. Mathematical modeling of transformation plasticity in steels. I: case of ideal-plastic phases. International Journal of Plasticity 5, 551–572.

Lechler, J., Merklein, M., 2008. Hot stamping of ultra strength steels as a key technology for lightweight construction. In: Materials Science and Technology (MS&T), Pittsburgh, Pennsylvania, pp. 1698–1709.

Lechler, J., 2009. Grundlegende Untersuchungen zur Beschreibung und Modellierung des Werkstoffverhaltens von presshärtbaren Bor-Manganstählen. Dr.-Ing. Dissertation, LFT, University of Erlangen-Nuremberg.

Lechler, J., Merklein, M., Geiger, M., 2009. Determination of thermal and mechanical material properties of ultra-high strength steels for hot stamping. Steel Research International 79 (2), 98–104.

Lenze, F.J., Banik, J., Sikora, S., 2008. Applications of hot formed parts for body in white. International Deep Drawing Research Group IDDRG, 511–519.

Lenze, F.J., Sikora, S., Banik, J., Sauer, D., 2008b. Development tendencies as to processing of press hardening under application of coated steel. In: 1st International Conference on Hot Sheet Metal Forming of High-Performance Steel, Kassel, Germany, pp. 15–21.

Lindkvist, G., Häggblad, H.Å., Oldenburg, M., 2009. Thermo-mechanical simulation of high temperature formblowing and hardening. In: 2nd International Conference on Hot Sheet Metal Forming of High-Performance Steel, Luleå, Sweden, pp. 247–254.

Maikranz-Valentin, M., Weidig, U., Schoof, U., Becker, H., Steinhoff, K., 2008. Components with optimised properties due to advanced thermo-mechanical process strategies in hot sheet metal forming. Steel Research International 79 (2), 92–97.

Merklein, M., Lechler, J., 2006. Investigation of the thermo-mechanical properties of hot stamping steels. Journal of Materials Processing Technology 177, 452–455.

Merklein, M., Lechler, J., 2008. Determination of material and process characteristics for hot stamping processes of quenchable ultra high strength steels with respect to a FE-based process design. SAE World Congress: Innovations in Steel and Applications of Advanced High Strength Steels for Automobile Structures, Paper No. 2008–0853.

Merklein, M., Lechler, J., Stöhr, T., 2008. Characterization of tribological and thermal properties of metallic coating for hot stamping boron-manganese steels. In: Proceedings of the 7th International Conference Coatings in Manufacturing Engineering, Chalkidiki, Greece, pp. 219–228.

Molinari, A.M., Ravichandran, G., 2005. Constitutive modeling of the high-strain-rate deformation in metals based on the evolution of an effective microstructural length. Mechanics of Materials 37, 737–752.

Mori, K., Maki, S., Tanaka, Y., 2009. Warm and hot stamping of ultra tensile strength steel sheets using resistance heating. CIRP Annals—Manufacturing Technology 54 (1), 209–212.

Mori, K., Ito, D., 2009. Prevention of oxidation in hot stamping of quenchable steel sheet by oxidation preventive oil. CIRP Annals—Manufacturing Technology 58 (1), 267–270.

Naderi, M., 2007. Hot stamping of ultra high strength steels. Doctoral Theses, RWTH Aachen.

Nemat-Nasser, S., 1999. Experimentally-based micromechanical modeling of metal plasticity with homogenization form micro-to-macro-scale properties. In: IUTAM Symposium on Micro- and Macrostructural Aspects of Thermoplasticity, pp. 101–113.

Neubauer, I., Hübner, K., Wicke, T., 2008. Thermo-mechanically coupled analysis: the next step in sheet metal forming simulation. In: 1st International Conference on Hot Sheet Metal Forming of High-Performance Steel, Kassel, Germany, pp. 275–283.

Neugebauer, R., Göschel, A., Sterzing, A., Schieck, F., 2009. Gas forming with integrated heat treatment for high performance steel—a solution approach for press hardened tubes and profiles. In: 2nd International Conference on Hot Sheet Metal Forming of High-Performance Steel, Luleå, Sweden, pp. 181–188.

N. N., 2008. Steels for hot stamping—very high strength steels. ArcelorMittal. www.arcelormittal.com.

N. N., 2009, Stahl-Informations-Zentrum. Stahl im Automobil, Leicht und sicher. www.stahl-info.de.

Norton, F.H., 1929. Creep of Steel at High Temperatures. McGraw-Hill, New York.

Oldenburg, M., Åkerström, P., Bergman, G., 2008. Simulation of the microstructure evolution in a press hardened component. In: 1st International Conference on Hot Sheet Metal Forming of High-Performance Steel, Kassel, Germany, pp. 3–13.

Olle, P., Behrens, B.A., Weilandt, K., Lange, F., 2008. Numerical modeling of phase transformation in hot stamping and deep drawing. In: The 9th International Conference on Technology of Plasticity, CIRP, pp. 1937–1942.

Paar, U., Becker, H.H., Alsmann, M., 2008. Press-hardened components from kassel—chances and challenges. In: 1st International Conference on Hot Sheet Metal Forming of High-Performance Steel, Kassel, Germany, pp. 153–163.

Patent GB1490535, 1977. Manufacturing a hardened steel article, Norrbottens Jaernverk AB.

Pawelski, O., 1964. Ein neues Gerät zum Messen des Reibungsbeiwertes bei plastischen Formänderungen. Stahl und Eisen, Nr. 20, 1233–1243.

Pellegrini, D., Lechler, J., Ghiotti, A., Bruschi, S., Merklein, M., 2009. Interlaboratory comparison of forming limit curves for hot stamping of high strength steels. Key Engineering Materials 410–411, 297–304.

Picas, I., Hernández, R., Casellas, D., Negona, C., Valls, I., 2008. Tool performance in cutting of hot stamped steels. In: 1st International Conference on Hot Sheet Metal Forming of High-Performance Steel, Kassel, Germany, pp. 179–189.

Siebel, E., Beisswänger, H., 1955. Tiefziehen. Hanser-Verlag, München.

So, H., Hoffmann, H., Golle, R., 2009. Blanking of press hardened ultra high strength steel. In: 2nd International Conference on Hot Sheet Metal Forming of High-Performance Steel, Luleå, Sweden, pp. 137–145.

Somani, M.C., Karjalainen, L.P., Eriksson, M., Oldenburg, M., 2001. Dimensional changes and microstructural evolution in a B-bearing steel in the simulated forming and quenching process. ISIJ International 4, 361–367.

Steinbeiss, H., So, H., Michelitsch, T., Hoffmann, H., 2007. Method for optimizing the cooling design of hot stamping tools. Production Engineering—Research and Development 1 (2), 149–155.

Stöhr, T., Merklein, M., Lechler, J., 2008. Determination of frictional and thermal characteristics for hot stamping with respect to a numerical process design. In: 1st International Conference on Hot Sheet Metal Forming of High-Performance Steel, Kassel, Germany, pp. 293–300.

Stöhr, T., Lechler, J., Merklein, M., 2009. Investigations on different strategies for influencing the microstructural properties with respect to partial hot stamping. In: 2nd International Conference on Hot Sheet Metal Forming of High-Performance Steel, Luleå, Sweden, pp. 273–281.

Stopp, R., Schaller, L., Lamprecht, K., Keupp, E., Deinzer, G., 2007. Warmblechumformung in der Automobil-Serienfertigung: Status, Trends und Potenziale. Tagungsband 2. Erlanger Workshop Warmblechumformung, Erlangen, Germany, 23–36.

Suehiro, M., Kusumi, K., Miyakoshi, T., Maki, J., Ohgami, M., 2003. Properties of aluminium-coated steels for hot-forming, Nippon Steel Technical Report No. 88, 16–21.

Tekkaya, A.E., Karbasian, H., Homberg, W., Kleiner, M., 2007. Thermo-mechanical coupled simulation of hot stamping components for process design. Annals of WGP XIV (1), 85–89.

Tong, L., Stahel, S., Hora, P., 2005. Modeling for the FE simulation of warm metal forming processes. In: The 6th International Conference and Workshop on Numerical Simulation of 3D Sheet Metal Forming Processes, pp. 625–629.

Yanagida, A., Azushima, A., 2009. Evaluation of coefficients of friction in hot stamping by hot flat drawing test. CIRP Annals—Manufacturing Technology 58, 247–250.

Yanagimoto, J., Oyamada, K., 2007. Mechanism of springback-free bending of high-strength steel sheets under warm forming conditions. CIRP Annals—Manufacturing Technology 56, 265–268.